# Corneal keratocytes, fibroblasts, and myofibroblasts exhibit distinct transcriptional profiles *in vitro*

Kara Poole[1,*], Krithika S. Iyer[2,3,*], David W. Schmidtke[2,3], W. Matthew Petroll[1,3,†], Victor D. Varner[2,3,†]

[1]Department of Ophthalmology, UT Southwestern Medical Center, Dallas, TX

[2]Department of Bioengineering, University of Texas at Dallas, Richardson, TX

[3]Department of Biomedical Engineering, UT Southwestern Medical Center, Dallas, TX

*These authors contributed equally to this work

†Corresponding authors

Address correspondence to V.D.V (vdv@utdallas.edu; victor.varner@utsouthwestern.edu) and W.M.P (matthew.petroll@utsouthwestern.edu)

Word Count: 6219

Funding: This work was supported by the NIH grants R01 EY013322, R01 EY030190, and P30 EY030413, as well as a Challenge grant from Research to Prevent Blindness.

Disclosure: K. Poole, None; K.S. Iyer, None; D.W. Schmidtke, None; W.M. Petroll, None; V.D. Varner, None

## ABSTRACT

**Purpose:** After stromal injury to the cornea, the release of growth factors and pro-inflammatory cytokines promotes the activation of quiescent keratocytes into a migratory fibroblast and/or fibrotic myofibroblast phenotype. Persistence of the myofibroblast phenotype can lead to corneal fibrosis and scarring, which are leading causes of blindness worldwide. This study aims to establish comprehensive transcriptional profiles for cultured corneal keratocytes, fibroblasts, and myofibroblasts to gain insights into the mechanisms through which these phenotypic changes occur.

**Methods:** Primary rabbit corneal keratocytes were cultured in either defined serum-free media (SF), fetal bovine serum (FBS) containing media, or in the presence of TGF-β1 to induce keratocyte, fibroblast, or myofibroblast phenotypes, respectively. Bulk RNA sequencing followed by bioinformatic analyses was performed to identify significant differentially expressed genes (DEGs) and enriched biological pathways for each phenotype.

**Results:** Genes commonly associated with keratocytes, fibroblasts, or myofibroblasts showed high relative expression in SF, FBS, or TGF-β1 culture conditions, respectively. Differential expression and functional analyses revealed novel DEGs for each cell type, as well as enriched pathways indicative of differences in proliferation, apoptosis, extracellular matrix (ECM) synthesis, cell-ECM interactions, cytokine signaling, and cell mechanics.

**Conclusions:** Overall, these data demonstrate distinct transcriptional differences among cultured corneal keratocytes, fibroblasts, and myofibroblasts. We have identified genes

23 and signaling pathways that may play important roles in keratocyte differentiation,
24 including many related to mechanotransduction and ECM biology. Our findings have
25 revealed novel molecular markers for each cell type, as well as possible targets for
26 modulating cell behavior and promoting physiological corneal wound healing.

## INTRODUCTION

The cornea is the soft tissue at the anterior aspect of the eye that is responsible for bending light towards the retina. It consists of three primary cellular layers: the epithelium, stroma, and endothelium, with the stroma accounting for 90% of the corneal thickness[1-3]. Throughout this stromal layer, corneal keratocytes[3, 4] are embedded within a highly organized extracellular matrix (ECM), consisting primarily of lamellae of aligned collagen fibrils[1, 2, 5]. In their quiescent state, keratocytes maintain the structure of the ECM[6-8], which is necessary for corneal transparency[9]. However, following injury, various growth factors, such as transforming growth factor beta 1 (TGF-β1), platelet derived growth factor-BB (PDGF-BB), and fibroblast growth factor (FGF), among others, enter the stromal space and initiate a wound healing response. During this process, corneal keratocytes transform into a repair phenotype that involves differentiation into either fibroblasts or myofibroblasts[4, 10, 11]. Corneal fibroblasts are characterized by increased proliferation and migration towards the site of injury[4, 12], whereas myofibroblasts adopt a contractile and fibrotic phenotype, in which they generate elevated traction forces, express alpha-smooth muscle actin (α-SMA), and secrete a variety of fibrotic ECM proteins[7, 13-21]. Myofibroblast differentiation is thought to be driven by signaling downstream of TGF-β1 and, in protracted cases, is associated with corneal haze and a loss of visual acuity[22, 23].

To study these stromal cell phenotypes *in vitro*, three distinct culture models have been established experimentally: 1) primary corneal keratocytes cultured in defined serum-free (SF) media to maintain a quiescent phenotype, 2) keratocytes cultured with fetal bovine

49 serum (FBS) to transform them into corneal fibroblasts, and 3) keratocytes cultured in the
50 presence of TGF-β1 to induce myofibroblast differentiation[24, 25]. Using these culture
51 conditions, previous studies have investigated the many phenotypic differences between
52 keratocytes, fibroblasts, and myofibroblasts, with several focusing on differences in the
53 morphology, motility, and mechanical behavior of these cells[19, 20, 26-28]. Many of these
54 studies have highlighted the importance of cell-ECM interactions, indicating how the
55 composition, structure, and mechanical properties of the ECM can regulate cell
56 contractility, migration, and ECM remodeling[19, 24, 27, 29, 30]. For example, the TGF-β1-
57 induced differentiation of myofibroblasts from quiescent corneal keratocytes is highly
58 sensitive to changes in ECM stiffness[20, 24]. However, it is still unclear how these cells
59 sense and transduce these biomechanical signals into changes in differentiation and
60 behavior.
61
62 An investigation of the global transcriptional profile associated with each of these cell
63 types could offer important information on the changes in gene expression associated
64 with keratocyte differentiation into fibroblasts and myofibroblasts. Such an approach also
65 offers the potential to pinpoint new target molecules within the signaling pathways that
66 precede each of these phenotypic changes. Here, we used bulk RNA sequencing (RNA-
67 seq) to establish comprehensive transcriptional profiles for cultured corneal keratocytes
68 (SF), fibroblasts (FBS), and myofibroblasts (TGF-β1). Differential gene expression and
69 functional analyses provided new insight into the mechanisms that regulate each of these

70 cell phenotypes. Of particular interest, we identified several differentially expressed genes

71 and pathways related to cell biomechanics and ECM remodeling.

72 **METHODS**

73 **Isolation and Cell Culture of Primary Rabbit Keratocytes**

74 Normal rabbit keratocytes (NRKs) were isolated from New Zealand white rabbit eyes (Pel-
75 Freez Biologicals, Rogers, AR) and cultured as described previously[25]. Briefly, after
76 removing the epithelium and endothelium, dissected corneal buttons were digested
77 overnight at 37°C in culture media containing 2.0 mg/mL collagenase (Gibco, Grand
78 Island, NY) and 0.5 mg/mL hyaluronidase (Worthington Biochemical Corporation,
79 Lakewood, NJ). The isolated cells were then centrifuge-pelleted, resuspended in defined
80 SF media containing Dulbecco's modified Eagle's medium (DMEM; Sigma-Aldrich, St.
81 Louis, MO) supplemented with 100 $\mu$M non-essential amino acids (Gibco, Grand Island,
82 NY), 100 $\mu$g/mL ascorbic acid (Sigma-Aldrich, St. Louis, MO), 1% RPMI vitamins solution
83 (Sigma-Aldrich, St. Louis, MO), and 1% antibiotic antimycotic solution (Sigma-Aldrich, St.
84 Louis, MO), and plated in 25 $cm^2$ tissue culture flasks. After 4 days of SF culture, first
85 passage NRKs were plated at a density of 30,000 cells/mL on glass coverslips coated
86 with 50 $\mu$g/mL type I collagen (Advanced BioMatrix, Carlsbad, CA)[31]. The cells were
87 allowed to attach to the substrates over 24 hr, then the culture media was swapped for
88 either defined SF media, SF media supplemented with 5 ng/mL TGF-β1 (Sigma-Aldrich,
89 St. Louis, MO), or DMEM containing 10% FBS (Sigma-Aldrich, St. Louis, MO). The cells
90 were then cultured for 5 days (with a media swap at 48 hr) for both SF and TGF-β1
91 conditions or for 3 days following exposure to FBS to account for the increased
92 proliferation rate in this condition.

93

94 **RNA Isolation and Sequencing**

95 Eight samples of total RNA were collected for each culture condition using the Aurum
96 Total RNA Mini Kit (Bio-Rad, Hercules, CA). Briefly, cells on collagen-coated glass
97 coverslips were washed twice with sterile phosphate-buffered saline (PBS) and lysed
98 using Aurum Total RNA Lysis Solution. The lysate was collected into sterile 1.5 mL tubes
99 and mixed with RNase-Free 70% ethanol before being added to Aurum RNA-Binding Mini
100 Columns. A series of centrifugation and low- and high-stringency solution washing steps
101 were performed before eluting the RNA from the columns using molecular biology grade
102 water. The concentration and purity of each sample were confirmed using a Thermo
103 Scientific NanoDrop One$^{C}$. For each culture condition, two experimental replicates (with
104 two biological and two technical replicates for each experiment) were sent to Novogene
105 Co. (Sacramento, CA) for bulk RNA-seq on Illumina platforms.

106

107 **Bioinformatic Analysis**

108 Initial bioinformatic analysis performed by Novogene included sample and data quality
109 control, mapping to the reference genome (Hisat2 v2.0.5), gene expression quantification
110 (featureCounts v1.5.0-p3), differential expression analysis (DESeq2 R package v1.20.0),
111 and enrichment analysis (clusterProfiler R package v3.8.1). The reference genome used
112 for sequence mapping was generated by the McDermott Center Next Generation
113 Sequencing Core at UT Southwestern Medical Center (Dallas, TX).

114

115 *Gene Expression Quantification*

116 FPKM (Fragments Per Kilobase of transcript per Million fragments mapped) values were
117 calculated based on the length and read count mapped to each gene. FPKM considers
118 the effects of both sequencing depth and gene length and is currently the most common
119 method for estimating gene expression levels. Principal component analysis (PCA) was
120 performed in MATLAB using FPKM values to compare the clustering of samples and
121 culture conditions. PCA is the method of algebraically reducing the dimensionality and
122 extracting significant components from several gene variables to evaluate differences
123 within a group and between different groups in a set of samples[32].
124
125 *Differential Expression Analysis*
126 Differential expression analysis was performed for the following comparisons: FBS vs.
127 SF, TGF-β1 vs. FBS, and TGF-β1 vs. SF. Parametric analysis of variance (ANOVA) with
128 Benjamini-Hochberg False Discovery Rate correction at $p = 0.05$ was performed on
129 normalized data to identify genes that were significantly differentially expressed between
130 groups (adjusted p-value $\leq 0.05$ and absolute value of log2(fold change) $\geq 1$). Heatmaps
131 were created in GraphPad Prism using normalized, log2-transformed FPKM values
132 (log2(FPKM+1)) to display relative expression levels across samples (columns) for sets
133 of differentially expressed genes (rows). To normalize expression levels, each sample's
134 gene expression value was adjusted by subtracting the average expression of that gene
135 across all samples, then dividing the result by the standard deviation of the gene's
136 expression. In addition, bar plots showing average FPKM values among the different
137 culture conditions were generated for selected genes of interest.

138

139 *Enrichment Analysis*

140 Sets of significant differentially expressed genes were further analyzed through Kyoto
141 Encyclopedia of Genes and Genomes (KEGG) enrichment analysis, and pathways with
142 padj $< 0.05$ were considered significantly enriched. Bar plots were generated in GraphPad
143 Prism to visualize pathway significance, the number of up- or downregulated genes
144 associated with each pathway, and the BRITE functional hierarchies under which each
145 pathway is classified. For a subset of significantly enriched KEGG pathways, volcano
146 plots were generated in GraphPad Prism to visualize the significance and log2(fold
147 change) of individual genes.

148

149 **Fluorescence Microscopy**

150 In other experiments, samples were fixed and stained for fluorescence microscopy.
151 Additional substrates for each culture condition were used for F-actin and nuclei labeling
152 and immunostaining for fibronectin, vimentin, or α-SMA to observe cytoskeletal
153 organization, morphological changes, and the presence of markers commonly associated
154 with each phenotype. Cells were fixed in 3% paraformaldehyde in PBS for 10 min at room
155 temperature, washed three times with PBS, then permeabilized in 0.5% Triton X-100 in
156 PBS for 15 min. The samples were then blocked with 1% bovine serum albumin fraction
157 V (Equitech-Bio, Kerrville, TX) in PBS for 1 hr at room temperature and incubated
158 overnight at 4°C with the primary antibody solution. The following primary antibodies were
159 used: anti-fibronectin (1:200 dilution; sc-18825; Santa Cruz Biotechnology, Dallas, TX),

160 anti-vimentin (1:200 dilution; sc-6260; Santa Cruz Biotechnology, Dallas, TX), and anti-
161 α-SMA (1:250 dilution; A5228; Sigma-Aldrich, St. Louis, MO). After washing three times,
162 samples were then incubated with Alexa Fluor conjugated secondary antibody, as well as
163 Alexa Fluor 546 phalloidin (Invitrogen, Waltham, MA) for 2 hr at room temperature,
164 followed by 4'-6-diamidino-2-phenylindole (DAPI; Invitrogen, Waltham, MA) for 20 min.
165 Imaging was performed on a Zeiss LSM 800 laser scanning confocal microscope using a
166 40×, NA 1.3, Oil DIC Plan-Apochromat objective.
167

168 **Western Blotting**

169 In other experiments, after rinsing twice with ice-cold, sterile PBS, protein was collected
170 from cells cultured in either SF, FBS, or TGF-β1 conditions using a lysis buffer solution
171 containing Pierce RIPA Buffer and Halt Protease & Phosphatase Inhibitor Cocktail
172 (Thermo Scientific, Waltham, MA). Sample lysates were mixed for 30 min at 4°C, then
173 centrifuged at 10,000G for 10 min at 4°C. Protein concentrations were measured using
174 the Microplate BCA Protein Assay Kit (Thermo Scientific, Waltham, MA) to determine load
175 volumes for 5 $\mu$g of total protein. Protein samples were subjected to SDS-PAGE
176 electrophoresis using Bio-Rad Mini-PROTEAN TGX Gels, then transferred to PVDF
177 membranes (Bio-Rad, Hercules, CA). Membranes were stained for total protein using
178 Ponceau S (Sigma-Aldrich, St. Louis, MO) and subsequently probed with primary
179 antibody followed by an anti-mouse IgG HRP-linked antibody (Cell Signaling, Danvers,
180 MA). The following primary antibodies were used: anti-aldehyde dehydrogenase 1-A1
181 (1:1000 dilution; sc-374149; Santa Cruz Biotechnology, Dallas, TX), anti-vimentin (1:1000

182 dilution; sc-6260; Santa Cruz Biotechnology, Dallas, TX), or anti-α-SMA (1:1000 dilution;
183 A5228; Sigma-Aldrich, St. Louis, MO). Colorimetric (total protein) or chemiluminescence
184 (target protein) imaging was performed using a GE Healthcare Amersham Imager 600
185 Series. In all cases, Image Studio software (version 5.2.5) was used to quantify protein
186 expression and the amount of target protein was normalized to the amount of total protein.
187 Statistical analysis was performed using GraphPad Prism 10. A one-way ANOVA with a
188 Tukey post-hoc test was used to compare group means, and a p-value of less than 0.05
189 was considered statistically significant.

190 **RESULTS**

191 **Distinct transcriptional profiles characterize corneal keratocytes in SF, FBS, and**
192 **TGF-β1 culture conditions.**

193 We conducted bulk RNA-seq experiments using primary NRKs cultured in defined SF
194 media, or in the presence of either FBS or exogenous TGF-β1. PCA showed distinct
195 transcriptional differences between cells in each culture condition (Fig. 1A). Technical and
196 experimental replicates clustered closely together in plots of PC1 vs. PC2, while the
197 clusters associated with each culture condition were clearly separated. This result
198 suggested the presence of a distinct gene expression profile for the cells within each
199 group. Subsequent differential expression analysis revealed numerous DEGs among the
200 different culture conditions (Fig. 1B). A comparison of FBS vs. SF contained the highest
201 total number of DEGs at 7693, followed by TGF-β1 vs. FBS at 5704, and TGF-β1 vs. SF
202 at 4430. DEGs present in more than one comparison were indicated by overlapping areas
203 on the Venn diagram (Fig. 1B). Cumulatively, 3174 genes were differentially expressed if
204 both FBS- and TGF-β1-treated cells were compared with SF, while 1311 genes were
205 differentially expressed among all three groups.

206

207 We also observed distinct differences in the number of up- and downregulated DEGs
208 when pairwise comparisons were made between culture conditions (Fig. 1C). A greater
209 fraction of DEGs was downregulated when comparing either FBS or TGF-β1 to SF,
210 whereas a slightly larger fraction of DEGs was upregulated when comparing TGF-β1 to
211 FBS. A heatmap of DEGs among all groups indicated further that a distinct transcriptional

212 profile was associated with each culture condition (Fig. 1D). Approximately 50% of these
213 DEGs had high relative expression in SF, while 28% and 22% showed high expression
214 in FBS and TGF-β1, respectively. Thus, the principal component, gene count, and
215 differential expression analyses illustrate distinct and significant differential gene
216 expression patterns between keratocytes cultured in SF media, FBS or TGF-β1.
217
218 **Markers associated with keratocytes, fibroblasts, and myofibroblasts are**
219 **differentially expressed between culture conditions.**
220 We then compared our transcriptional data with molecular markers known to be
221 associated with corneal keratocytes, fibroblasts, and myofibroblasts. Proteoglycans and
222 corneal crystallins known to be important for corneal transparency[2, 33, 34], such as
223 keratocan (KERA), mimecan (OGN), decorin (DCN), lumican (LUM), aldehyde
224 dehydrogenase 1 family member A1 (ALDH1A1), and transketolase (TKT), showed high
225 relative expression in SF culture (Fig. 2A). In a consistent manner, analysis of western
226 blot data confirmed elevated ALDH1A1 levels when comparing SF to either FBS or TGF-
227 β1, indicating a quiescent keratocyte phenotype in this culture condition (Fig. 2B).
228
229 Following injury, corneal fibroblasts exhibit an increased proliferative and migratory
230 phenotype, so we also compared levels of expression for genes associated with
231 proliferation and cell-ECM interactions in FBS-treated cells[4, 35]. We observed significant
232 increases in the expression of proliferative markers, such as Ki-67 (MKI67)[36, 37] and
233 proliferating cell nuclear antigen (PCNA)[38, 39], as compared to either SF or TGF-β1 (Fig.

234 2A). In addition, genes encoding vimentin (VIM)[40], a cytoskeletal intermediate filament,
235 and tenascin C (TNC)[41], an ECM protein synthesized in repair tissue, also exhibited
236 elevated expression following treatment with FBS. Western blots confirmed increased
237 levels of vimentin in FBS; however, vimentin was also detected at elevated levels in TGF-
238 β1-treated cells (Fig. 2C, S1), a result consistent with previous reports of vimentin
239 expression in myofibroblasts[42].
240
241 We also observed elevated expression of alpha-smooth muscle actin (α-SMA; ACTA2),
242 which incorporates into stress fibers and plays an important role in the increased
243 contractility of myofibroblasts, in both FBS and TGF-β1 as compared to SF (Fig. 2A). In
244 addition, since myofibroblasts have been shown to secrete fibrotic ECM proteins,
245 including biglycan (BGN)[43-46] and fibronectin (FN1)[47], we compared the expression levels
246 of BGN and FN1, which were most upregulated upon treatment with TGF-β1. We also
247 observed increased expression of α5 integrin (ITGA5) in both FBS and TGF-β1 (Fig. 2A).
248 Integrin α5β1 is a receptor for fibronectin[48, 49] and, in previous work, has been shown to
249 be upregulated in both corneal fibroblasts and myofibroblasts[6, 50]. Additionally, consistent
250 with our FN1 expression data, we observed the highest levels of fibronectin
251 immunofluorescence in the presence of TGF-β1 (Fig. 2D), which, as other studies have
252 shown previously[18], is indicative of a myofibroblast phenotype is this culture condition.
253
254 Overall, our RNA-seq data are broadly consistent with known molecular markers for
255 corneal keratocytes, fibroblasts, and myofibroblasts, with SF conditions supporting a

256 keratocyte phenotype, FBS-containing media inducing a fibroblast phenotype, and
257 treatment with TGF-β1 eliciting a myofibroblast phenotype. Even so, genes encoding
258 some fibroblast and myofibroblast markers, such as ITGA5 and ACTA2, were expressed
259 at similar levels in both FBS and TGF-β1 culture conditions, indicating overlap between
260 the gene expression profiles of fibroblasts and myofibroblasts.
261

262 **Diverse pathways associated with signal transduction and cellular processes such**
263 **as cell growth and death, cell-ECM and cell-cell interactions are enriched in the**
264 **comparisons of fibroblasts and myofibroblasts to keratocytes.**

265 KEGG analysis revealed an enrichment of several pathways associated with either signal
266 transduction in TGF-β1-treated myofibroblasts or proliferation in FBS-treated fibroblasts,
267 when compared to keratocytes in SF conditions (Fig. 3). In the presence of FBS (as
268 compared to SF), genes were primarily upregulated in pathways related to translation,
269 replication and repair, and cell growth and death. Among these, we observed significant
270 enrichment of the ribosome and ribosome biogenesis pathways, as well as the DNA
271 replication and cell cycle pathways, suggesting a shift towards increased protein
272 synthesis and cell proliferation upon treatment with FBS (Fig. 3A). In addition, significant
273 changes in expression were observed for genes involved in the PI3K-Akt and Rap1
274 signaling pathways, as well as those associated with ECM-receptor interactions. These
275 pathways have roles in diverse processes related to proliferation and apoptosis[51-53],
276 adhesion and migration, and cell-cell and cell-matrix interactions[54-57].
277

278 In contrast, the focal adhesion, regulation of actin cytoskeleton, ECM-receptor interaction,
279 and Rap1 signaling KEGG pathways were significantly enriched in the comparison of
280 TGF-β1 to SF, suggesting changes in cytoskeletal organization, cell motility and
281 contractility, and cell-ECM interactions among cultured myofibroblasts (Fig. 3B). Other
282 enriched pathways were broadly related to either cytokine activity (e.g., cytokine-cytokine
283 receptor interaction, as well as TGF-β, JAK-STAT, and TNF signaling pathways) or
284 proliferation and apoptosis (e.g., PI3K-Akt, p53, MAPK, and Hippo signaling pathways).
285
286 Strikingly, when TGF-β1-treated myofibroblasts were compared to fibroblasts (as
287 opposed to keratocytes), many of the same KEGG pathways, especially those related to
288 proliferation, cell-ECM interactions, and cytokine activity, were enriched (Fig. 3C).
289 Relative to cells cultured in FBS, TGF-β1 elicited a downregulation of genes associated
290 with the cell cycle and DNA replication pathways, as well as an upregulation of genes in
291 the ECM-receptor interaction pathway. In addition, the cellular senescence pathway,
292 which has been associated with aging, tumor suppression, and wound healing[58, 59], was
293 also enriched in this comparison. Taken together, these data were suggestive of lower
294 rates of proliferation and a greater emphasis on cell-ECM interactions in TGF-β1-treated
295 myofibroblasts.
296
297 **Genes related to proliferation and migration are significantly upregulated in**
298 **fibroblasts as compared to keratocytes.**

299 Numerous genes in the DNA replication, cell cycle, and PI3K-Akt signaling KEGG
300 pathways were differentially expressed in fibroblasts as compared to keratocytes (Fig.
301 4A-C). Elevated expression was observed for several key genes that encode parts of the
302 DNA replication machinery, including PCNA, MCM2-7, and several DNA polymerase
303 subunits such as POLA2 and POLE2-3[60]. There was also an increase in the expression
304 of several genes associated with the PI3K-Akt signaling pathway, such as the receptor
305 tyrosine kinase MET and the MAP Kinase MAP2K1, which are involved in regulation of
306 proliferation[61, 62], and several cyclin dependent kinases (CDKs) such as CDK2 and CDK4,
307 which are key regulators of cell cycle progression[63]. The upregulation of these genes was
308 indicative of an increased proliferative phenotype for cultured corneal fibroblasts.
309
310 Numerous DEGs within the ECM-receptor interaction and Rap1 signaling pathways also
311 indicated a shift toward a migratory phenotype (Fig. 4D-E). Ras-related protein Rap-1b
312 (RAP1B) encodes for a small GTPase that regulates cell adhesion, migration, and
313 polarity[54, 55, 64]. We observed increased expression of RAP1B, along with an upregulation
314 of β-actin (ACTB), which also plays a key role in cell motility[65]. In addition, focal adhesion-
315 related genes, such as talin (TLN2), and genes that regulate actin polymerization, like
316 profilin (PFN2)[66], were downregulated following treatment with FBS. Changes in cell-ECM
317 interactions were indicated by shifts in the expression of different integrin subunits and
318 many of their corresponding ECM binding partners. This included the downregulation of
319 various collagens (COL1, COL2, COL4, COL6) and the upregulation of tenascin C (TNC),
320 which has been shown to modulate cell adhesion and migration[67, 68]. Consistently, many

321 of the genes encoding integrin subunits that bind to tenascin, such as ITGA8, ITGAV,
322 ITGB1, and ITGB3, were also upregulated. Taken together, these transcriptional changes
323 support an increased proliferative and migratory phenotype in cultured corneal fibroblasts.
324

325 **Proliferation related genes are significantly downregulated, while genes involved**
326 **in cell-ECM interactions and cytokine signaling are upregulated in myofibroblasts**
327 **compared to fibroblasts.**

328 We observed similar differences in proliferation- and motility-related genes when
329 comparing fibroblasts and myofibroblasts. Multiple genes in the DNA replication and cell
330 cycle pathways were differentially expressed between these groups, with lower levels of
331 expression in myofibroblasts indicating a less proliferative phenotype (Fig. 5A-B).
332 Interestingly, genes involved in cell cycle arrest and evasion of apoptosis, such as the
333 cyclin dependent kinase inhibitors 1A and 2B (CDKN1A, CDKN2B), as well as B-cell
334 lymphoma 2 (BCL2), were upregulated in TGF-β1-treated myofibroblasts (Fig. 5C-D)[63,
335 69-71].
336

337 TGF-β1 has been attributed to the induction of ECM synthesis in myofibroblasts[72]. Here,
338 several ECM genes, including fibronectin (FN1), tenascin N (TNN), various collagens
339 (COL1A1, COL1A2, COL2A1, COL9A3), and some of the integrin subunits (e.g., ITGA11,
340 ITGAV, ITGB3) associated with these ECM proteins[57, 73], exhibited increased expression
341 levels in myofibroblasts compared to fibroblasts (Fig. 5E). Interestingly, the expression of
342 chondroadherin (CHAD), which has been previously shown to promote the adhesion of

343 chondrocytes, fibroblasts, and osteoblasts, was also significantly upregulated in
344 myofibroblasts[74, 75]. In addition, a different gene involved in cell motility – hyaluronan
345 mediated motility receptor (HMMR) – was downregulated in myofibroblasts relative to
346 fibroblasts[76, 77].
347
348 This comparison also revealed significant differences in the expression of genes related
349 to cytokine signaling (Fig. 5F), including (perhaps not surprisingly) several TGF-β family
350 genes (Fig. 5G). Numerous genes encoding TGF-β superfamily ligands, such as growth
351 differentiation factors (GDFs) 6-7 and 9-11, as well as transforming growth factor beta 2
352 and 3 (TGFB2, TGFB3)[78], were upregulated in myofibroblasts. We also noted differences
353 in the expression of genes related to cell inflammatory responses, including the
354 interleukins IL1A, IL1B, and IL6, as well as the colony stimulating factors CSF1 and CSF3.
355 These genes were downregulated in myofibroblasts as compared to fibroblasts, which
356 are believed to be the cell type responsible for triggering innate immune responses in the
357 cornea[79].
358
359 In addition, we observed differential expression of several genes associated with TGF-β
360 signaling, some of which encode proteins that are known to modulate TGF-β activity (Fig.
361 5G). This included the upregulation of two proteoglycans, decorin (DCN) and fibromodulin
362 (FMOD), along with thrombospondin type 1 domain containing 4 (THSD4), fibrillin 1
363 (FBN1), and latent transforming growth factor beta binding protein 1 (LTBP1)[80].
364

365 **Genes related to cell-ECM interactions and mechanotransduction are differentially**
366 **expressed in myofibroblasts compared to keratocytes and fibroblasts.**
367 Many of the significantly enriched KEGG pathways identified in the comparison of
368 myofibroblasts to keratocytes were associated with cell-ECM interactions and
369 mechanotransduction. These included the ECM-receptor interaction, focal adhesion,
370 regulation of actin cytoskeleton, TGF-β signaling, and Hippo signaling pathways (Fig. 6A-
371 E). Additional KEGG enrichment analysis focused on genes that were significantly
372 upregulated in myofibroblasts revealed significant enrichment of the vascular smooth
373 muscle contraction pathway (Fig. 6F). Consistent with the KEGG analysis, a closer look
374 at the differential gene set for the comparison of myofibroblasts to keratocytes identified
375 many DEGs related to ECM, cell-ECM adhesion, cell-cell interaction, Hippo signaling,
376 actomyosin contractility, and growth factor signaling. Using these categories, genes of
377 interest selected from the highlighted KEGG pathways and the broader differential gene
378 set were classified based on their function and were further evaluated for their relative
379 expression across all three culture conditions (Fig. 7A).
380
381 Multiple collagens were highly expressed in the myofibroblasts compared to keratocytes
382 and fibroblasts. One of the most notable collagens that was significantly upregulated in
383 myofibroblasts was collagen type XI alpha 1 chain (COL11A1) (Fig. 7A, 7B). Interestingly,
384 several other ECM-related genes, such as integrin binding sialoprotein (IBSP), secreted
385 phosphoprotein 1 (SPP1), and leucine rich repeat containing 15 (LRRC15), and integrins
386 such as integrin subunit alpha 11 (ITGA11) were also significantly upregulated in

387 myofibroblasts (Fig. 7A, 7B, Table S1). IBSP is a structural bone matrix protein and SPP1
388 encodes for osteopontin, known to be important in TGF-β1-induced myofibroblast
389 differentiation[81, 82]. LRRC15 is a membrane protein known to be involved in ECM binding
390 and as a marker for cancer associated myofibroblasts in lung, breast, and other tumors[83-
391 85]. Our data revealed a very significant upregulation of LRRC15 in the presence of TGF-
392 β1, compared to cells cultured in both SF and FBS conditions.
393
394 Within the family of genes related to growth factor signaling, a significant upregulation
395 was observed for TGFB1 and TGFB3 in the presence of exogenous TGF-β1 compared
396 to SF (Fig. 7A). Previous work has suggested that TGF-β1 induces the secretion of PDGF
397 as part of an autocrine signaling loop which regulates myofibroblast differentiation[86].
398 However, it is still unknown which PDGF subunits are involved in this process. Here, our
399 data shows a significant upregulation of PDGFA in myofibroblasts relative to keratocytes
400 and fibroblasts, while PDGFB is downregulated relative to keratocytes (Fig. 7A).
401
402 In the comparison of myofibroblasts to keratocytes, DEGs involved in Hippo signaling also
403 stood out due to known crosstalk between this pathway and TGF-β signaling and its
404 association with mechanotransduction[87-89]. Our data revealed differential expression of
405 several Hippo signaling related genes, including connective tissue growth factor (CTGF)
406 and TEA domain transcription factor 4 (TEAD4), which were significantly upregulated in
407 myofibroblasts compared to keratocytes (Fig. 7A, 7C). Interestingly, TEAD4 showed even
408 higher expression in FBS-treated conditions relative to TGF-β1. CTGF, which was most

409 highly expressed in TGF-β1 conditions, is a downstream target of yes-associated protein
410 (YAP) activation, a known mechanosensor[90]. AMOT, encoding for angiomotin, has been
411 known to sequester YAP and TAZ to the cytoplasm, thus reducing the nuclear localization
412 of YAP/TAZ and their downstream effects[91]. Our data indicates that AMOT is significantly
413 downregulated in TGF-β1-treated conditions compared to SF, suggesting nuclear
414 localization of YAP/TAZ.
415
416 Several genes involved in actomyosin contractility, such as myosin light/heavy chains and
417 ACTA2, were also upregulated in myofibroblasts as compared to the quiescent
418 keratocytes. ACTA2, a gene encoding for alpha-smooth muscle actin (α-SMA), was
419 significantly upregulated in both fibroblasts and myofibroblasts compared to keratocytes
420 (Fig. 7A, 7D). α-SMA is an important marker for TGF-β1-induced myofibroblast
421 differentiation[25] and previous studies have shown that the expression of α-SMA in corneal
422 keratocytes is influenced by ECM mechanics[19, 20, 26].
423
424 Another interesting family of genes our data revealed to be differentially expressed in
425 myofibroblasts were the thrombospondins 1,2 and 4 (THBS 1,2,4), known to have the
426 ability to bind to various ECM proteins and play a key role in cell-ECM and cell-cell
427 interactions[92] (Fig. 7A). THBS1 specifically, was significantly upregulated in
428 myofibroblasts compared to keratocytes (Fig. 7A, 7D) and is known to be important for
429 TGF-β1-induced myofibroblast differentiation[93].
430

## Discussion

While many phenotypic differences between corneal keratocytes, fibroblasts, and myofibroblasts have been well documented both *in vivo* and *in vitro*, the transcriptional changes and signaling pathways regulating these differences remain a subject of ongoing research. Improving our understanding of keratocyte differentiation from a genomic perspective could have important implications in corneal wound healing and fibrosis. For this study, we used a 2D *in vitro* model in which corneal keratocytes were cultured in either SF conditions, media containing FBS, or SF media with exogeneous TGF-β1 to produce either corneal keratocytes, fibroblasts, or myofibroblasts, respectively. We then performed bulk RNA sequencing to obtain a global view of the transcriptional differences between each of these cell types. Differential gene expression and functional analyses provided insight into the mechanisms regulating the phenotypic changes associated with each cell type, as well as novel molecular markers and potential targets for modulating cell behavior and differentiation.

Over the years, many previous studies have documented key phenotypic differences between corneal keratocytes, fibroblasts, and myofibroblasts. These include changes in proliferation, ECM synthesis, cell morphology, cytoskeletal organization, and mechanical activity (e.g., adhesion, migration, contractility, etc.)[7, 12, 20, 21, 24-26, 94-96]. Our analyses revealed unique transcriptional profiles for each cell type, which likely underlie these phenotypic differences, since many of the DEGs and enriched signaling pathways were related to proliferation, ECM, and cell mechanics. Among these pathways, we also

453 identified several individual genes that may warrant further investigation to determine their
454 functional significance in the differentiation of keratocytes into fibroblasts and
455 myofibroblasts.
456
457 Following injury or surgery, the transformation of quiescent keratocytes into proliferative
458 and migratory fibroblasts is an integral step in the process of corneal wound healing[28, 97].
459 Our RNA-seq data suggest that the increased proliferation observed among corneal
460 fibroblasts is associated with the upregulation of genes involved in the DNA replication,
461 cell cycle, and PI3K-Akt signaling pathways. This proliferative gene expression signature
462 includes the upregulation of key genes, such as E2F1/2 and CDK2/4/6, in fibroblasts as
463 compared to keratocytes and myofibroblasts. These genes, as well as their associated
464 signaling pathways, may be of further interest as potential targets for accelerating cell
465 repopulation during corneal wound healing or promoting stromal regeneration[98].
466
467 Although the differentiation of myofibroblasts is important for wound closure, a persistent
468 myofibroblast phenotype can lead to protracted corneal fibrosis[97, 99]. Our transcriptional
469 analyses indicated that, although genes associated with proliferation were
470 downregulated, corneal myofibroblasts also appeared to adopt an apoptotic-resistant
471 phenotype associated with pathological wound healing[100, 101], as indicated by changes in
472 the cell cycle, cellular senescence, PI3K-Akt, and p53 signaling pathways. Genes of
473 interest within these pathways included BCL2, which was upregulated in myofibroblasts
474 compared to both keratocytes and fibroblasts. Due to its role in suppressing apoptosis,

475 BCL2 has been studied for its therapeutic potential in cancer and during wound healing
476 in other tissues[71, 102, 103]. In general, the evasion of apoptosis by myofibroblasts is
477 considered a hallmark of fibrotic disease, making therapeutic modulation of the cell cycle
478 and apoptosis of interest in a range of pathologies[100, 104, 105]. In the case of corneal wound
479 healing, targeting genes related to apoptosis could be used to support the timely
480 disappearance of myofibroblasts after wound closure to help prevent a fibrotic response.
481
482 ECM synthesis and remodeling by corneal keratocytes is important for maintaining the
483 stromal composition and structure that allows for the optical transparency of the tissue.
484 This ECM-maintenance phenotype is disrupted when keratocytes differentiate into
485 fibroblasts and myofibroblasts, a process that changes the types and quantities of ECM
486 proteins produced by the cells[45]. Although previous work has identified several collagens
487 and proteoglycans that are differentially expressed among the different stromal cell types,
488 our data provides a more comprehensive profiling of the many ECM-related genes
489 associated with the matrisome[106, 107]. This includes ECM structural proteins (e.g.,
490 collagens, proteoglycans, glycoproteins), cell-ECM receptors (e.g., integrins), ECM-
491 modifying enzymes, and ECM-binding growth factors/cytokines. Altered expression of
492 genes encoding these proteins can produce changes in matrix composition and structure
493 that impact a wide range of cell behaviors, including proliferation, cytoskeletal
494 organization, and mechanical activity[107].
495

496 How the myofibroblast matrisome differs from that of keratocytes and corneal fibroblasts
497 is of particular interest because a key component of the myofibroblast phenotype is the
498 synthesis of an unorganized, fibrotic ECM. Our results are consistent with previous data
499 indicating that the expression of various keratocyte-associated proteoglycans, such as
500 KERA, OGN, and DCN, is reduced in myofibroblasts, while the expression of ECM genes
501 associated with fibrosis (e.g., COL3A1, FN1) is elevated[47]. Our analyses also revealed
502 additional ECM-related genes that were highly upregulated in myofibroblasts and may
503 impact their fibrotic phenotype, including osteopontin (SPP1 or OPN) and integrin binding
504 sialoprotein (IBSP). Each of these genes are primarily expressed within bone matrix, but
505 there is also evidence supporting their role in wound healing and fibrosis in other tissue
506 types[81, 82, 108-112]. OPN expression is important in TGF-β1-induced myofibroblast
507 differentiation within dermal and cardiac fibroblasts and is thought to be a promising
508 therapeutic target for cardiac fibrosis[81, 82]. In addition, OPN knockout mice exhibit delayed
509 corneal wound healing following an incisional injury, which was associated with lower
510 levels of TGF-β1 expression and fewer myofibroblasts[110].
511
512 Changes in ECM composition within the corneal stroma likely also elicit changes in cell
513 behavior via interactions with integrin-containing receptors. Tenascin C (TNC) and
514 fibronectin (FN1), which have been investigated extensively for their involvement in
515 inflammation, wound healing, and tissue remodeling[97, 112, 113], were found to be highly
516 expressed in corneal fibroblasts and myofibroblasts, respectively. Tenascin C modulates
517 cell adhesion and migration via several integrin receptors, including α8β1 and αvβ1, the

518 subunits of which exhibited elevated gene expression among our cultured fibroblasts.
519 These increases in the expression of TNC and its associated integrin subunits may work
520 together to support the anti-adhesive and pro-migratory phenotypes of corneal fibroblasts,
521 which, along with proliferation, are critical in the early response to corneal injury. In
522 contrast to tenascin C, fibronectin promotes robust cell adhesion to the ECM. Previous
523 work has reported increased fibronectin expression for myofibroblasts, as well as
524 changes in the composition and localization of focal adhesions[20, 21]. Consistent with these
525 data, we observed an upregulation in cultured myofibroblasts of many genes encoding
526 focal adhesion proteins, such as vinculin (VCL), talin (TLN2), and paxillin (PXN). The
527 development of mature focal adhesions is thought to influence the elevated mechanical
528 phenotype associated with myofibroblasts, including increased contractility and traction
529 force generation[21].
530
531 Overall, our data have identified distinct ECM-related gene expression profiles for
532 keratocytes, fibroblasts, and myofibroblasts, which likely contribute to their associated
533 phenotypes. Gene expression by corneal keratocytes promotes a quiescent, ECM-
534 maintenance phenotype, while the altered expression of ECM-related genes promotes a
535 migratory phenotype for fibroblasts and a fibrotic, contractile phenotype for
536 myofibroblasts. How ECM composition and cell-ECM interactions impact corneal wound
537 healing remains a topic of great interest, since ECM structure and composition are
538 important determinants of corneal transparency.
539

540 *In vitro* experiments, particularly those employing three-dimensional collagen matrices,
541 have also highlighted the importance of ECM mechanics and stiffness in regulating
542 corneal cell migration, contractility, and ECM reorganization[19, 24, 27, 29, 30]. Furthermore,
543 TGF-β1-induced differentiation of myofibroblasts from quiescent keratocytes is highly
544 sensitive to changes in the mechanical properties of the ECM[20, 24]. In the presence of
545 TGF-β1, keratocytes cultured on softer, uncompressed 3D collagen gels, exhibit fewer
546 stress fibers and reduced expression of α-SMA compared to cells cultured on stiffer, more
547 compressed collagen matrices[14, 19, 94, 95, 114, 115]. Other *in vitro* studies using
548 polyacrylamide gels of varying stiffnesses have shown that corneal keratocytes cultured
549 on stiffer substrata exhibit elevated levels of myofibroblast differentiation in response to
550 TGF-β1, as indicated by an increased number of α-SMA positive cells. This elevated
551 differentiation is also accompanied by changes in both the contractile behavior of the cells
552 and the subcellular localization of focal adhesions[20, 21].
553
554 Given that ECM stiffness is recognized as a significant factor in myofibroblast
555 differentiation, we hypothesized that mechanotransduction-related genes and signaling
556 pathways would be upregulated following culture in the presence of TGF-β1. Indeed, our
557 RNA-seq analyses identified an enrichment of pathways related to cell contractility (e.g.,
558 vascular smooth muscle contraction) and mechanotransduction (e.g., Hippo signaling),
559 which include several genes that may contribute to the mechanical differences observed
560 between myofibroblasts and keratocytes. For instance, within the Hippo signaling
561 pathway, we observed changes in the expression of angiomotin (AMOT) and multiple

562 SMADs among myofibroblasts, which are associated with the subcellular localization and
563 activity of YAP/TAZ[91]. Consistent with these data, in previous work, YAP and TAZ have
564 been reported to help regulate myofibroblast differentiation in human corneal
565 fibroblasts[116]. In addition, AMOT has been shown to bind YAP and TAZ, sequester them
566 to the cytoplasm, and thus suppress YAP/TAZ-mediated transcription[91]. In our
567 observation, the downregulation of AMOT among myofibroblasts is consistent with
568 elevated YAP/TAZ activity. This idea is also supported by the increased expression of
569 CTGF, a downstream transcriptional target of YAP activation[90], in cultured
570 myofibroblasts.
571
572 Alpha-smooth muscle actin (α-SMA) expression is a key molecular marker for
573 myofibroblasts. The incorporation of α-SMA into stress fibers is considered a hallmark of
574 myofibroblast differentiation and has been shown to play a significant role in increased
575 contractility and force generation of these cells[13]. Within the vascular smooth muscle
576 contraction pathway, ACTA2, the gene encoding α-SMA, was significantly upregulated in
577 myofibroblasts, as compared to keratocytes. Consistent with previous work, TGF-β1-
578 treated myofibroblasts also contained α-SMA positive stress fibers (Fig. S2A) and
579 western blots showed high α-SMA protein levels relative to keratocytes (Fig. S2B).
580 Interestingly, an even higher level of ACTA2 expression was measured for corneal
581 fibroblasts, although we did not observe the incorporation of α-SMA into stress fibers
582 among cells in this culture condition (Fig. S2A), and western blots showed lower α-SMA
583 protein levels relative to myofibroblasts (Fig. S2B). The RNA-seq data may indicate an

584 important transcriptional difference in ACTA2 expression between corneal fibroblasts and
585 myofibroblasts; however, it is also a possibility that time-varying changes in ACTA2
586 expression levels contribute to this finding. Furthermore, the western blot data suggest
587 that α-SMA protein levels do not correlate with ACTA2 transcriptional levels when
588 comparing fibroblasts and myofibroblasts, which may indicate potential post-
589 transcriptional or translational control mechanisms.
590
591 Taken together, our findings using bulk RNA sequencing provide the first comprehensive
592 differential gene expression profile for cultured corneal keratocytes, fibroblasts, and
593 myofibroblasts. In our initial analysis, we have identified genes and signaling pathways
594 that may play important roles in keratocyte differentiation and the maintenance of these
595 distinct phenotypes. In the future, this sequencing data set can continue to be a resource
596 to identify potential targets for guiding keratocyte differentiation and behavior and serve
597 as a foundation for future studies investigating the influence of substratum stiffness on
598 corneal keratocyte gene expression. Additional experiments targeting specific genes of
599 interest can further reveal the biological and functional significance of these findings as
600 they relate to the broader fields of wound healing, fibrosis, and tissue engineering.
601
602 **AUTHOR CONTRIBUTIONS**
603 KP, KSI, VDV, WMP, and DWS conceived the study and designed experiments. KP and
604 KSI conducted all experiments and analyzed all experimental data. All authors discussed

605 and interpreted results. KP, KSI, VDV, and WMP wrote the manuscript with feedback from

606 all authors.

607

608 **ACKNOWLEDGMENTS**

609 The authors would also like to thank the members of the Varner, Petroll, and Schmidtke

610 labs for their many helpful discussions and comments.

611

612 **REFERENCES**

613 1. Meek, K.M. and C. Boote, *The use of X-ray scattering techniques to quantify the orientation and*
614 *distribution of collagen in the corneal stroma.* Prog Retin Eye Res, 2009. **28**(5): p. 369-92.
615 2. Meek, K.M., *Corneal collagen-its role in maintaining corneal shape and transparency.* Biophys Rev,
616 2009. **1**(2): p. 83-93.
617 3. Nishida, T., et al., *The network structure of corneal fibroblasts in the rat as revealed by scanning*
618 *electron microscopy.* Invest Ophthalmol Vis Sci, 1988. **29**(12): p. 1887-90.
619 4. Fini, M.E., *Keratocyte and fibroblast phenotypes in the repairing cornea.* Prog Retin Eye Res, 1999.
620 **18**(4): p. 529-51.
621 5. Worthen, D.M., *Histology of the Human Eye.* Archives of Ophthalmology, 1972. **88**: p. 234-234.
622 6. Beales, M.P., et al., *Proteoglycan Synthesis by Bovine Keratocytes and Corneal Fibroblasts:*
623 *Maintenance of the Keratocyte Phenotype in Culture.* Investigative Ophthalmology & Visual
624 Science, 1999. **40**(8): p. 1658-1663.
625 7. Jester, J.V., et al., *Corneal keratocytes: in situ and in vitro organization of cytoskeletal contractile*
626 *proteins.* Invest Ophthalmol Vis Sci, 1994. **35**(2): p. 730-43.
627 8. Zieske, J.D., S.R. Guimarães, and A.E. Hutcheon, *Kinetics of keratocyte proliferation in response to*
628 *epithelial debridement.* Exp Eye Res, 2001. **72**(1): p. 33-9.
629 9. Hassell, J.R. and D.E. Birk, *The molecular basis of corneal transparency.* Exp Eye Res, 2010. **91**(3):
630 p. 326-35.
631 10. Imanishi, J., et al., *Growth factors: importance in wound healing and maintenance of transparency*
632 *of the cornea.* Prog Retin Eye Res, 2000. **19**(1): p. 113-29.
633 11. Wilson, S.E., et al., *The corneal wound healing response: cytokine-mediated interaction of the*
634 *epithelium, stroma, and inflammatory cells.* Prog Retin Eye Res, 2001. **20**(5): p. 625-37.
635 12. Petroll, W.M., et al., *Corneal Fibroblast Migration Patterns During Intrastromal Wound Healing*
636 *Correlate With ECM Structure and Alignment.* Invest Ophthalmol Vis Sci, 2015. **56**(12): p. 7352-61.
637 13. Jester, J.V., et al., *Expression of α-smooth muscle (α-SM) actin during corneal stromal wound*
638 *healing.* Investigative Ophthalmology and Visual Science, 1995. **36**(5): p. 809-819.
639 14. Jester, J.V. and J. Ho-Chang, *Modulation of cultured corneal keratocyte phenotype by growth*
640 *factors/cytokines control in vitro contractility and extracellular matrix contraction.* Exp Eye Res,
641 2003. **77**(5): p. 581-92.

15. Myrna, K.E., S.A. Pot, and C.J. Murphy, *Meet the corneal myofibroblast: the role of myofibroblast transformation in corneal wound healing and pathology.* Vet Ophthalmol, 2009. **12 Suppl 1**(Suppl 1): p. 25-7.
16. Nakamura, K., *Interaction between injured corneal epithelial cells and stromal cells.* Cornea, 2003. **22**(7 Suppl): p. S35-47.
17. Kurosaka, H., et al., *Transforming growth factor-beta 1 promotes contraction of collagen gel by bovine corneal fibroblasts through differentiation of myofibroblasts.* Invest Ophthalmol Vis Sci, 1998. **39**(5): p. 699-704.
18. Jester, J.V., et al., *Transforming Growth Factorβ–Mediated Corneal Myofibroblast Differentiation Requires Actin and Fibronectin Assembly.* Investigative Ophthalmology & Visual Science, 1999. **40**(9): p. 1959-1967.
19. Petroll, W.M. and M. Miron-Mendoza, *Mechanical interactions and crosstalk between corneal keratocytes and the extracellular matrix.* Experimental Eye Research, 2015. **133**: p. 49-57.
20. Maruri, D.P., et al., *ECM Stiffness Controls the Activation and Contractility of Corneal Keratocytes in Response to TGF-β1.* Biophys J, 2020. **119**(9): p. 1865-1877.
21. Maruri, D.P., et al., *Signaling Downstream of Focal Adhesions Regulates Stiffness-Dependent Differences in the TGF-β1-Mediated Myofibroblast Differentiation of Corneal Keratocytes.* Frontiers in Cell and Developmental Biology, 2022. **10**.
22. Wilson, S.E., *Corneal myofibroblast biology and pathobiology: Generation, persistence, and transparency.* Experimental Eye Research, 2012. **99**: p. 78-88.
23. Jester, J.V., W.M. Petroll, and H.D. Cavanagh, *Corneal stromal wound healing in refractive surgery: the role of myofibroblasts.* Progress in Retinal and Eye Research, 1999. **18**(3): p. 311-356.
24. Kim, A., et al., *Growth Factor Regulation of Corneal Keratocyte Differentiation and Migration in Compressed Collagen Matrices.* Investigative Ophthalmology & Visual Science, 2010. **51**(2): p. 864-875.
25. Jester, J.V., et al., *Induction of α-smooth muscle actin expression and myofibroblast transformation in cultured corneal keratocytes.* Cornea, 1996. **15**(5): p. 505-516.
26. Lakshman, N. and W.M. Petroll, *Growth Factor Regulation of Corneal Keratocyte Mechanical Phenotypes in 3-D Collagen Matrices.* Investigative Opthalmology & Visual Science, 2012. **53**(3): p. 1077.
27. Kim, A., et al., *Corneal Stromal Cells use both High- and Low-Contractility Migration Mechanisms in 3-D Collagen Matrices.* Experimental cell research, 2012. **318**: p. 741-52.
28. Andresen, J.L., T. Ledet, and N. Ehlers, *Keratocyte migration and peptide growth factors: the effect of PDGF, bFGF, EGF, IGF-I, aFGF and TGF-beta on human keratocyte migration in a collagen gel.* Curr Eye Res, 1997. **16**(6): p. 605-13.
29. Kim, A., N. Lakshman, and W.M. Petroll, *Quantitative assessment of local collagen matrix remodeling in 3-D Culture: The role of Rho kinase.* Experimental Cell Research, 2006. **312**(18): p. 3683-3692.
30. Miron-Mendoza, M., et al., *The Role of Thrombin and Cell Contractility in Regulating Clustering and Collective Migration of Corneal Fibroblasts in Different ECM Environments.* Investigative Ophthalmology & Visual Science, 2015. **56**(3): p. 2079-2090.
31. Kivanany, P., et al., *An In Vitro Model for Assessing Corneal Keratocyte Spreading and Migration on Aligned Fibrillar Collagen.* Journal of Functional Biomaterials, 2018. **9**(4): p. 54.
32. Ringnér, M., *What is principal component analysis?* Nature Biotechnology, 2008. **26**(3): p. 303-304.
33. Hassell, J.R., et al., *Proteoglycan changes during restoration of transparency in corneal scars.* Archives of Biochemistry and Biophysics, 1983. **222**(2): p. 362-369.
34. Jester, J.V., *Corneal crystallins and the development of cellular transparency.* Semin Cell Dev Biol, 2008. **19**(2): p. 82-93.

690 35. Mohan, R.R., et al., *Apoptosis, necrosis, proliferation, and myofibroblast generation in the stroma*
691 *following LASIK and PRK.* Exp Eye Res, 2003. **76**(1): p. 71-87.
692 36. McKay, T.B., et al., *Extracellular Vesicles Secreted by Corneal Epithelial Cells Promote Myofibroblast*
693 *Differentiation.* Cells, 2020. **9**(5): p. 1080.
694 37. Zixian, D., et al., *Small incision lenticule extraction (SMILE) and femtosecond laser LASIK:*
695 *comparison of corneal wound healing and inflammation.* British Journal of Ophthalmology, 2014.
696 **98**(2): p. 263.
697 38. binte M. Yusoff, N.Z., et al., *Isolation and Propagation of Human Corneal Stromal Keratocytes for*
698 *Tissue Engineering and Cell Therapy.* Cells, 2022. **11**(1): p. 178.
699 39. Gan, L., P. Fagerholm, and S. Ekenbark, *Expression of proliferating cell nuclear antigen in corneas*
700 *kept in long term culture.* Acta Ophthalmol Scand, 1998. **76**(3): p. 308-13.
701 40. Wilson, S.E., *The Yin and Yang of Mesenchymal Cells in the Corneal Stromal Fibrosis Response to*
702 *Injury: The Cornea as a Model of Fibrosis in Other Organs.* Biomolecules, 2022. **13**(1).
703 41. Latvala, T., et al., *Expression of cellular fibronectin and tenascin in the rabbit cornea after excimer*
704 *laser photorefractive keratectomy: a 12 month study.* British Journal of Ophthalmology, 1995.
705 **79**(1): p. 65.
706 42. Chaurasia, S.S., et al., *Dynamics of the expression of intermediate filaments vimentin and desmin*
707 *during myofibroblast differentiation after corneal injury.* Experimental Eye Research, 2009. **89**(2):
708 p. 133-139.
709 43. Funderburgh, J.L., et al., *Proteoglycan expression during transforming growth factor beta -induced*
710 *keratocyte-myofibroblast transdifferentiation.* J Biol Chem, 2001. **276**(47): p. 44173-8.
711 44. Funderburgh, J.L., et al., *Decorin and biglycan of normal and pathologic human corneas.*
712 Investigative Ophthalmology & Visual Science, 1998. **39**(10): p. 1957-1964.
713 45. Funderburgh, J.L., M.M. Mann, and M.L. Funderburgh, *Keratocyte phenotype mediates*
714 *proteoglycan structure: a role for fibroblasts in corneal fibrosis.* J Biol Chem, 2003. **278**(46): p.
715 45629-37.
716 46. Massoudi, D., F. Malecaze, and S.D. Galiacy, *Collagens and proteoglycans of the cornea:*
717 *importance in transparency and visual disorders.* Cell and Tissue Research, 2016. **363**(2): p. 337-
718 349.
719 47. Garana, R.M.R., et al., *Radial keratotomy: II. Role of the myofibroblast in corneal wound*
720 *contraction.* Investigative Ophthalmology and Visual Science, 1992. **33**(12): p. 3271-3282.
721 48. Welch, M.P., G.F. Odland, and R.A. Clark, *Temporal relationships of F-actin bundle formation,*
722 *collagen and fibronectin matrix assembly, and fibronectin receptor expression to wound*
723 *contraction.* J Cell Biol, 1990. **110**(1): p. 133-45.
724 49. Schumacher, S., et al., *Structural insights into integrin α(5)β(1) opening by fibronectin ligand.* Sci
725 Adv, 2021. **7**(19).
726 50. Masur, S.K., J.K. Cheung, and S. Antohi, *Identification of integrins in cultured corneal fibroblasts*
727 *and in isolated keratocytes.* Investigative Ophthalmology & Visual Science, 1993. **34**(9): p. 2690-
728 2698.
729 51. Engelman, J.A., J. Luo, and L.C. Cantley, *The evolution of phosphatidylinositol 3-kinases as*
730 *regulators of growth and metabolism.* Nat Rev Genet, 2006. **7**(8): p. 606-19.
731 52. Kim, D. and J. Chung, *Akt: versatile mediator of cell survival and beyond.* J Biochem Mol Biol, 2002.
732 **35**(1): p. 106-15.
733 53. Chen, K., et al., *The role of the PI3K/AKT signalling pathway in the corneal epithelium: recent*
734 *updates.* Cell Death Dis, 2022. **13**(5): p. 513.
735 54. Bos, J.L., *Linking Rap to cell adhesion.* Curr Opin Cell Biol, 2005. **17**(2): p. 123-8.
736 55. Boettner, B. and L. Van Aelst, *Control of cell adhesion dynamics by Rap1 signaling.* Curr Opin Cell
737 Biol, 2009. **21**(5): p. 684-93.

56. Bosman, F.T. and I. Stamenkovic, *Functional structure and composition of the extracellular matrix.* J Pathol, 2003. **200**(4): p. 423-8.
57. van der Flier, A. and A. Sonnenberg, *Function and interactions of integrins.* Cell Tissue Res, 2001. **305**(3): p. 285-98.
58. Childs, B.G., et al., *Cellular senescence in aging and age-related disease: from mechanisms to therapy.* Nat Med, 2015. **21**(12): p. 1424-35.
59. Muñoz-Espín, D. and M. Serrano, *Cellular senescence: from physiology to pathology.* Nat Rev Mol Cell Biol, 2014. **15**(7): p. 482-96.
60. Waga, S. and B. Stillman, *The DNA replication fork in eukaryotic cells.* Annu Rev Biochem, 1998. **67**: p. 721-51.
61. Trusolino, L., A. Bertotti, and P.M. Comoglio, *MET signalling: principles and functions in development, organ regeneration and cancer.* Nat Rev Mol Cell Biol, 2010. **11**(12): p. 834-48.
62. Organ, S.L. and M.S. Tsao, *An overview of the c-MET signaling pathway.* Ther Adv Med Oncol, 2011. **3**(1 Suppl): p. S7-s19.
63. Łukasik, P., M. Załuski, and I. Gutowska, *Cyclin-Dependent Kinases (CDK) and Their Role in Diseases Development-Review.* Int J Mol Sci, 2021. **22**(6).
64. Wilson, J.M., et al., *Differences in the Phosphorylation-Dependent Regulation of Prenylation of Rap1A and Rap1B.* J Mol Biol, 2016. **428**(24 Pt B): p. 4929-4945.
65. Bunnell, T.M., et al., *β-Actin specifically controls cell growth, migration, and the G-actin pool.* Mol Biol Cell, 2011. **22**(21): p. 4047-58.
66. Ding, Z. and P. Roy, *Profilin-1 versus profilin-2: two faces of the same coin?* Breast Cancer Res, 2013. **15**(3): p. 311.
67. Jones, F.S. and P.L. Jones, *The tenascin family of ECM glycoproteins: structure, function, and regulation during embryonic development and tissue remodeling.* Dev Dyn, 2000. **218**(2): p. 235-59.
68. Midwood, K.S. and G. Orend, *The role of tenascin-C in tissue injury and tumorigenesis.* J Cell Commun Signal, 2009. **3**(3-4): p. 287-310.
69. Bartkova, J., et al., *Cell-cycle regulatory proteins in human wound healing.* Archives of Oral Biology, 2003. **48**(2): p. 125-132.
70. Reed, J.C., *Bcl-2 and the regulation of programmed cell death.* J Cell Biol, 1994. **124**(1-2): p. 1-6.
71. Ruvolo, P.P., X. Deng, and W.S. May, *Phosphorylation of Bcl2 and regulation of apoptosis.* Leukemia, 2001. **15**(4): p. 515-22.
72. Wilson, S.E., *Corneal myofibroblasts and fibrosis.* Exp Eye Res, 2020. **201**: p. 108272.
73. Degen, M., et al., *Tenascin-W is a novel marker for activated tumor stroma in low-grade human breast cancer and influences cell behavior.* Cancer Res, 2007. **67**(19): p. 9169-79.
74. Mizuno, M., R. Fujisawa, and Y. Kuboki, *Bone chondroadherin promotes attachment of osteoblastic cells to solid-state substrates and shows affinity to collagen.* Calcif Tissue Int, 1996. **59**(3): p. 163-7.
75. Camper, L., D. Heinegârd, and E. Lundgren-Akerlund, *Integrin alpha2beta1 is a receptor for the cartilage matrix protein chondroadherin.* J Cell Biol, 1997. **138**(5): p. 1159-67.
76. Tolg, C., et al., *Hyaluronan and RHAMM in wound repair and the "cancerization" of stromal tissues.* Biomed Res Int, 2014. **2014**: p. 103923.
77. Hinneh, J.A., et al., *The role of RHAMM in cancer: Exposing novel therapeutic vulnerabilities.* Front Oncol, 2022. **12**: p. 982231.
78. Wrana, J.L., *Signaling by the TGFβ superfamily.* Cold Spring Harb Perspect Biol, 2013. **5**(10): p. a011197.
79. Fukuda, K., *Corneal fibroblasts: Function and markers.* Experimental Eye Research, 2020. **200**: p. 108229.

80. Soo, C., et al., *Differential expression of fibromodulin, a transforming growth factor-beta modulator, in fetal skin development and scarless repair.* Am J Pathol, 2000. **157**(2): p. 423-33.
81. Lenga, Y., et al., *Osteopontin expression is required for myofibroblast differentiation.* Circ Res, 2008. **102**(3): p. 319-27.
82. Abdelaziz Mohamed, I., et al., *Osteopontin: A Promising Therapeutic Target in Cardiac Fibrosis.* Cells, 2019. **8**(12).
83. Purcell, J.W., et al., *LRRC15 Is a Novel Mesenchymal Protein and Stromal Target for Antibody-Drug Conjugates.* Cancer Res, 2018. **78**(14): p. 4059-4072.
84. Krishnamurty, A.T., et al., *LRRC15(+) myofibroblasts dictate the stromal setpoint to suppress tumour immunity.* Nature, 2022. **611**(7934): p. 148-154.
85. Krishnamurty, A., et al., *1434 TGFβ-dependent LRRC15<sup>+</sup> myofibroblasts dictate the tumor fibroblast setpoint to promote cancer immunotherapy resistance.* Journal for ImmunoTherapy of Cancer, 2023. **11**(Suppl 1): p. A1597-A1597.
86. Jester, J.V., et al., *TGFβ Induced Myofibroblast Differentiation of Rabbit Keratocytes Requires Synergistic TGFβ, PDGF and Integrin Signaling.* Experimental Eye Research, 2002. **75**(6): p. 645-657.
87. Attisano, L. and J.L. Wrana, *Signal integration in TGF-β, WNT, and Hippo pathways.* F1000Prime Rep, 2013. **5**: p. 17.
88. Chang, Y.C., et al., *Hippo Signaling-Mediated Mechanotransduction in Cell Movement and Cancer Metastasis.* Front Mol Biosci, 2019. **6**: p. 157.
89. Cobbaut, M., et al., *Dysfunctional Mechanotransduction through the YAP/TAZ/Hippo Pathway as a Feature of Chronic Disease.* Cells, 2020. **9**(1): p. 151.
90. Raghunathan, V.K., et al., *Involvement of YAP, TAZ and HSP90 in contact guidance and intercellular junction formation in corneal epithelial cells.* PLoS One, 2014. **9**(10): p. e109811.
91. Chan, S.W., et al., *Hippo pathway-independent restriction of TAZ and YAP by angiomotin.* J Biol Chem, 2011. **286**(9): p. 7018-26.
92. Lahav, J., *The functions of thrombospondin and its involvement in physiology and pathophysiology.* Biochim Biophys Acta, 1993. **1182**(1): p. 1-14.
93. Bradshaw, A.D., *Chapter 15 - Regulation of Cell Behavior by Extracellular Proteins*, in *Principles of Tissue Engineering (Fourth Edition)*, R. Lanza, R. Langer, and J. Vacanti, Editors. 2014, Academic Press: Boston. p. 279-290.
94. Lakshman, N., A. Kim, and W.M. Petroll, *Characterization of corneal keratocyte morphology and mechanical activity within 3-D collagen matrices.* Experimental Eye Research, 2010. **90**(2): p. 350-359.
95. Karamichos, D., N. Lakshman, and W.M. Petroll, *Regulation of Corneal Fibroblast Morphology and Collagen Reorganization by Extracellular Matrix Mechanical Properties.* Investigative Ophthalmology & Visual Science, 2007. **48**(11): p. 5030-5037.
96. Iyer, K.S., et al., *ECM stiffness modulates the proliferation but not the motility of primary corneal keratocytes in response to PDGF-BB.* Experimental Eye Research, 2022. **220**: p. 109112.
97. Kamil, S. and R.R. Mohan, *Corneal stromal wound healing: Major regulators and therapeutic targets.* Ocul Surf, 2021. **19**: p. 290-306.
98. Lagali, N., *Corneal Stromal Regeneration: Current Status and Future Therapeutic Potential.* Curr Eye Res, 2020. **45**(3): p. 278-290.
99. Desai, V.D., H.C. Hsia, and J.E. Schwarzbauer, *Reversible Modulation of Myofibroblast Differentiation in Adipose-Derived Mesenchymal Stem Cells.* PLOS ONE, 2014. **9**(1): p. e86865.
100. Hinz, B. and D. Lagares, *Evasion of apoptosis by myofibroblasts: a hallmark of fibrotic diseases.* Nat Rev Rheumatol, 2020. **16**(1): p. 11-31.

101. McElhinney, K., M. Irnaten, and C. O'Brien, *p53 and Myofibroblast Apoptosis in Organ Fibrosis.* International Journal of Molecular Sciences, 2023. **24**(7): p. 6737.
102. Qian, S., et al., *The role of BCL-2 family proteins in regulating apoptosis and cancer therapy.* Front Oncol, 2022. **12**: p. 985363.
103. Wilkinson, H.N. and M.J. Hardman, *Senescence in Wound Repair: Emerging Strategies to Target Chronic Healing Wounds.* Front Cell Dev Biol, 2020. **8**: p. 773.
104. Wu, Y.S., et al., *Cell Cycle Dysregulation and Renal Fibrosis.* Front Cell Dev Biol, 2021. **9**: p. 714320.
105. Rosenwald, A., et al., *The proliferation gene expression signature is a quantitative integrator of oncogenic events that predicts survival in mantle cell lymphoma.* Cancer Cell, 2003. **3**(2): p. 185-97.
106. Naba, A., et al., *The extracellular matrix: Tools and insights for the "omics" era.* Matrix Biology, 2016. **49**: p. 10-24.
107. Hynes, R.O. and A. Naba, *Overview of the matrisome--an inventory of extracellular matrix constituents and functions.* Cold Spring Harb Perspect Biol, 2012. **4**(1): p. a004903.
108. Icer, M.A. and M. Gezmen-Karadag, *The multiple functions and mechanisms of osteopontin.* Clin Biochem, 2018. **59**: p. 17-24.
109. Sumioka, T., et al., *Tenascins and osteopontin in biological response in cornea.* Ocul Surf, 2023. **29**: p. 131-149.
110. Miyazaki, K.-i., et al., *Corneal Wound Healing in an Osteopontin-Deficient Mouse.* Investigative Ophthalmology & Visual Science, 2008. **49**(4): p. 1367-1375.
111. Moorman, H.R., et al., *Osteopontin: A Key Regulator of Tumor Progression and Immunomodulation.* Cancers, 2020. **12**(11): p. 3379.
112. Saika, S., et al., *Modulation of Smad signaling by non-TGFβ components in myofibroblast generation during wound healing in corneal stroma.* Exp Eye Res, 2016. **142**: p. 40-8.
113. Varkoly, G., et al., *Expression Pattern of Tenascin-C, Matrilin-2, and Aggrecan in Diseases Affecting the Corneal Endothelium.* Journal of Clinical Medicine, 2022. **11**(20): p. 5991.
114. Raghunathan, V.K., et al., *Tissue and cellular biomechanics during corneal wound injury and repair.* Acta Biomaterialia, 2017. **58**: p. 291-301.
115. Dreier, B., et al., *Substratum Compliance Modulates Corneal Fibroblast to Myofibroblast Transformation.* Investigative Ophthalmology & Visual Science, 2013. **54**(8): p. 5901-5907.
116. Muppala, S., et al., *YAP and TAZ are distinct effectors of corneal myofibroblast transformation.* Exp Eye Res, 2019. **180**: p. 102-109.

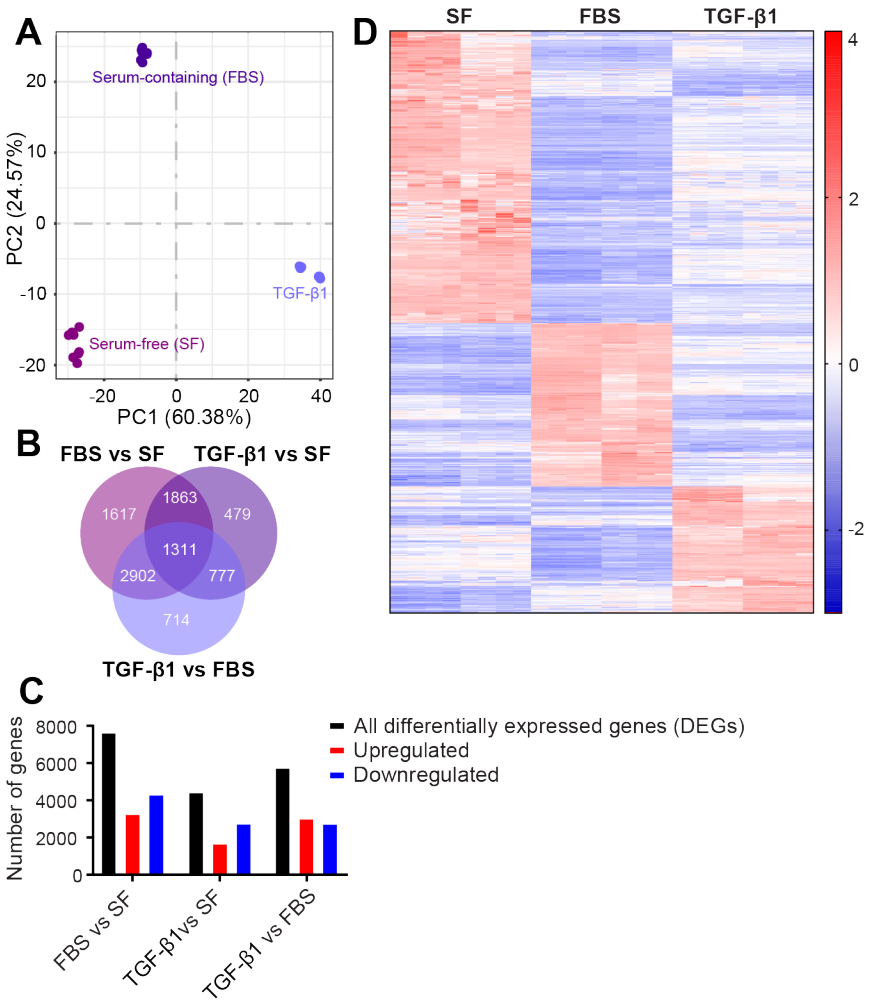


**Figure 1. Distinct transcriptional profiles characterize corneal keratocytes in SF, FBS, and TGF-β1 culture conditions.** (A) Principal component analysis (PCA) of transcriptional differences between corneal keratocytes cultured in defined serum-free (SF) media, FBS, or TGF-β1. Principal component (PC) 1 and PC2, account for 60.38% and 24.57% respectively, of the variability among these groups. Analysis was performed using normalized, log2- transformed FPKM values. (B) Venn diagram shows the number of significant differentially expressed genes (DEGs) in each comparison. DEGs with an adjusted p-value (padj) ≤ 0.05 and | log2(fold change) | ≥ 1 were considered significant. (C) Bar plot represents the number of DEGs either up- or downregulated in each comparison. (D) Heatmap of normalized, log2-transformed FPKM values (log2(FPKM+1)) for genes that were differentially expressed across all three culture conditions. Red color indicates genes with high relative expression levels and blue color indicates genes with lower expression levels.

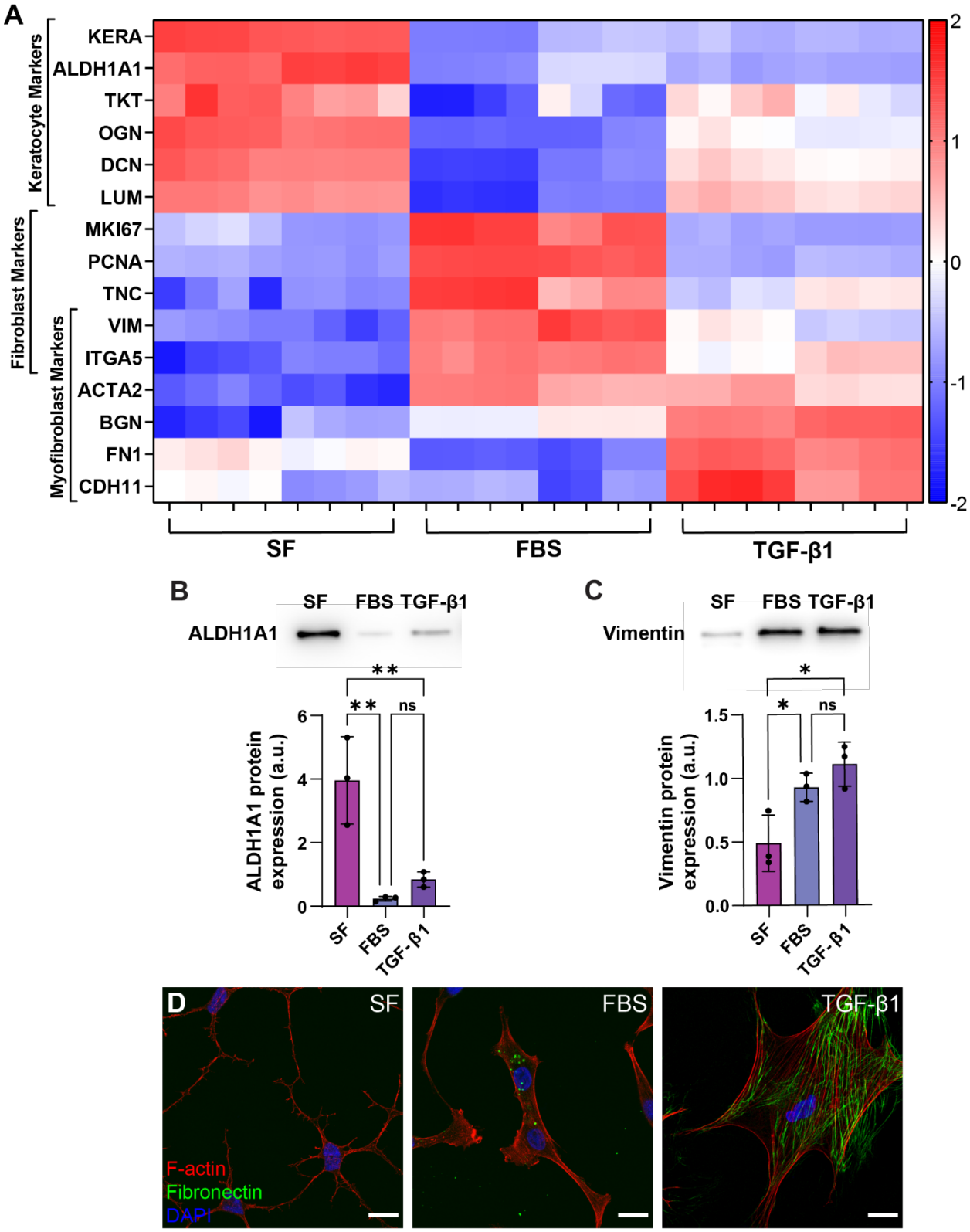


**Figure 2. Markers associated with keratocytes, fibroblasts, and myofibroblasts are differentially expressed between culture conditions.** (A) Heatmap of normalized,

885 log2-transformed FPKM values (log2(FPKM+1)) for known keratocyte, fibroblast, and
886 myofibroblast markers. Red color indicates genes with high relative expression levels and
887 blue color indicates genes with lower expression levels. (B, C) Representative western
888 blot and quantification of (B) ALDH1A1 as a marker for keratocytes and (C) Vimentin as
889 a marker for fibroblasts and myofibroblasts. Quantification of target protein expression
890 was normalized to total protein and reported in arbitrary units (a.u.). Error bars represent
891 mean ± s.d. for 3 experimental replicates. A one-way ANOVA with a Tukey post-hoc test
892 was used to compare group means (*, $p < 0.05$; **, $p < 0.01$). (D) Confocal overlay images
893 of F-actin, fibronectin, and DAPI staining for corneal keratocytes cultured in SF conditions,
894 or in the presence of FBS or TGF-β1. Scale bar = 20 $\mu$m.

895

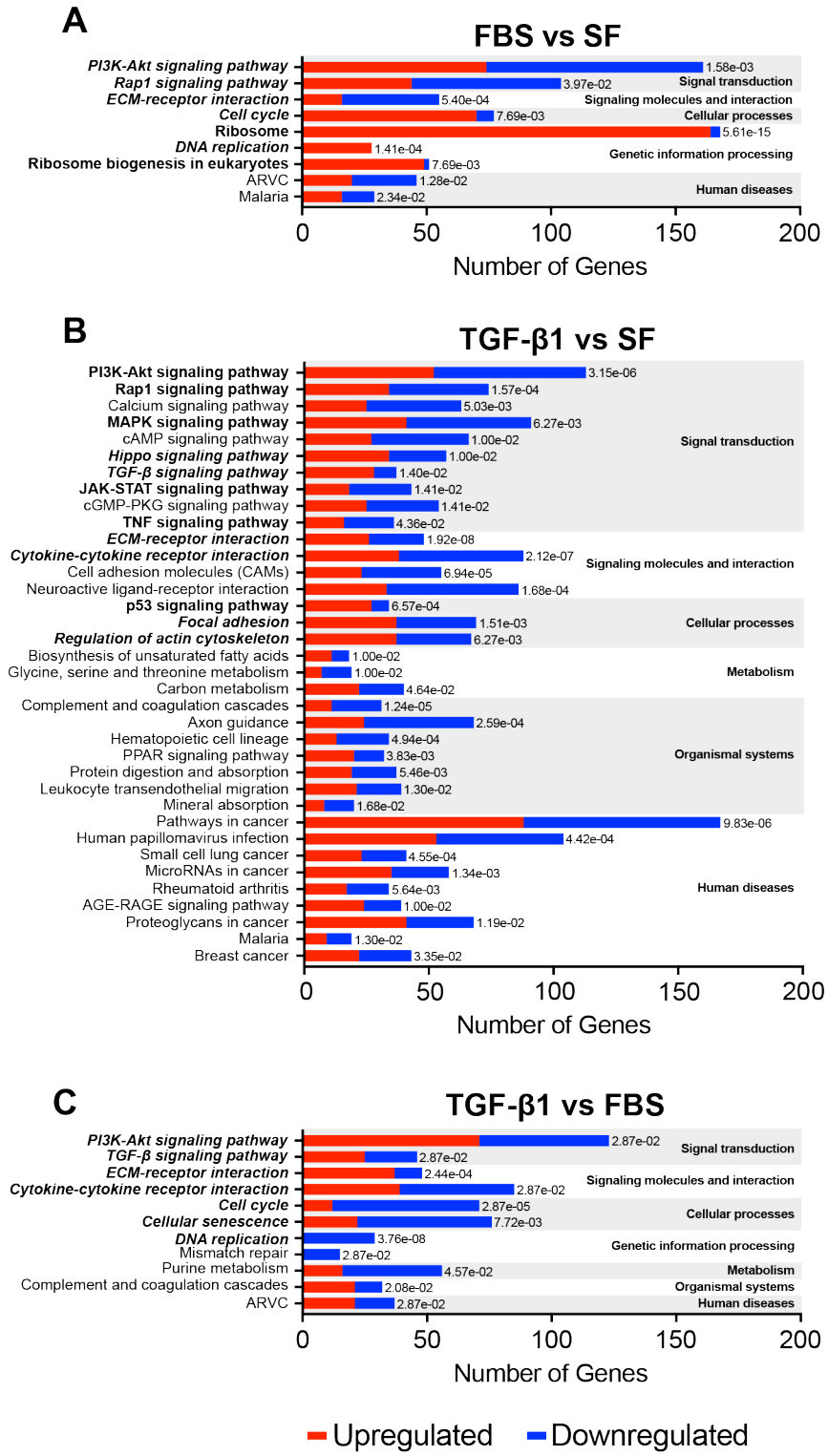


**Figure 3. KEGG pathways associated with proliferation are significantly enriched in the comparison of FBS vs. SF, while pathways associated with signal transduction are enriched in the comparison of TGF-β1 vs. SF.** Bars represent the number of genes either up- or downregulated in each significantly enriched KEGG

901 pathway from the comparisons of (A) FBS vs. SF, (B) TGF-β1 vs. SF, and (C) TGF-β1
902 vs. FBS. In each comparison, the alternating grey and white bars differentiate the KEGG
903 pathways grouped together based on their associated function, as indicated on the right
904 of each box. Within each group, pathways have been arranged in order of significance,
905 from most to least significant. KEGG pathways with a padj $< 0.05$ were considered
906 significant. Pathways of particular interest are highlighted in bold type.

907

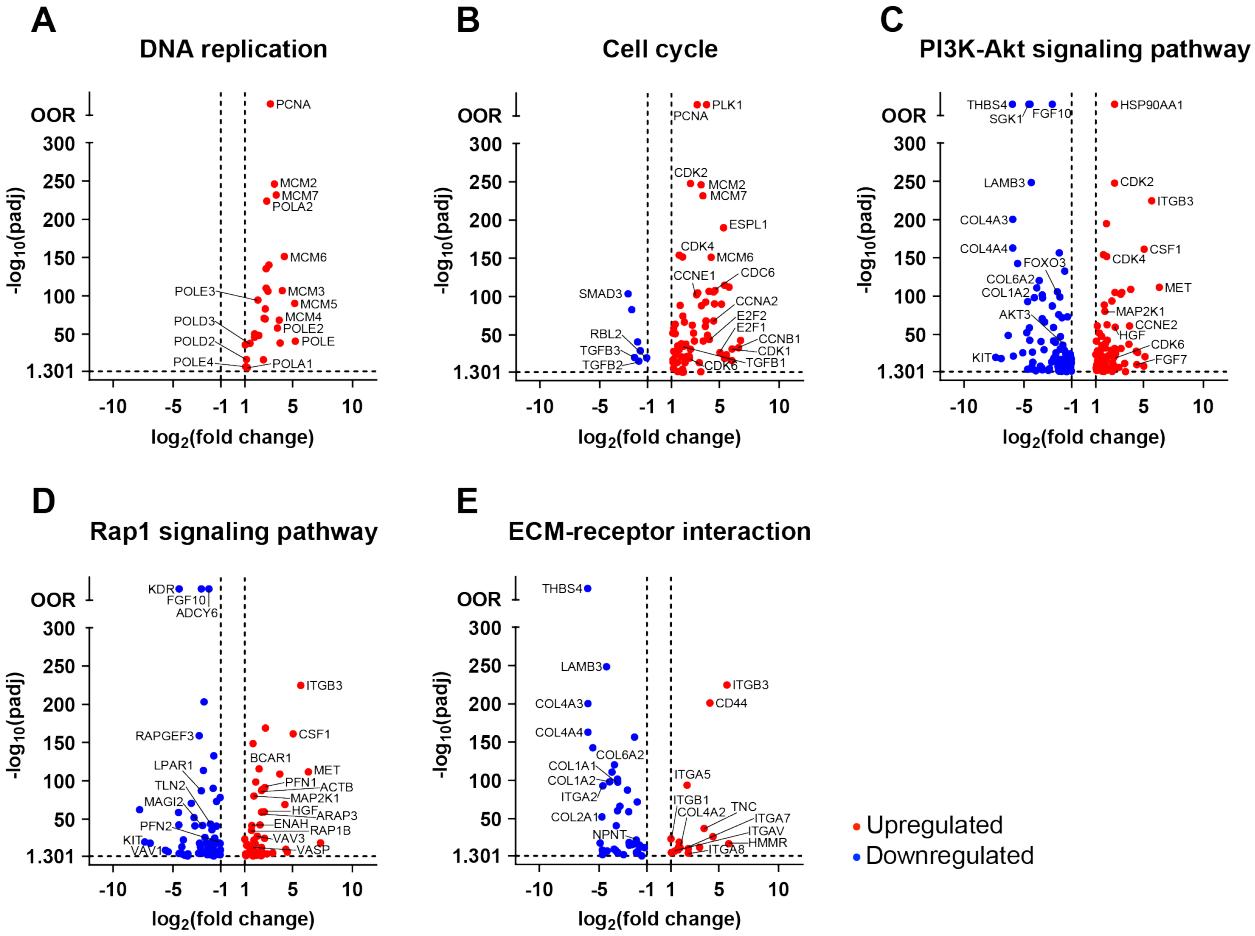


**Figure 4. FBS vs. SF: Genes related to a migratory and proliferative phenotype are significantly upregulated in fibroblasts as compared to quiescent keratocytes.** (A-E) Volcano plots represent individual genes significantly up- or downregulated within selected KEGG pathways from the comparison of fibroblasts to keratocytes. Genes with padj ≤ 0.05 (horizontal dashed line) and l log2(fold change) l ≥ 1 (vertical dashed lines) were considered significant. Red dots indicate genes that were upregulated in fibroblasts while blue dots indicate downregulated genes. Genes generally associated with FBS induced fibroblast phenotypes and several other significant genes with high padj values or fold changes have been labeled.

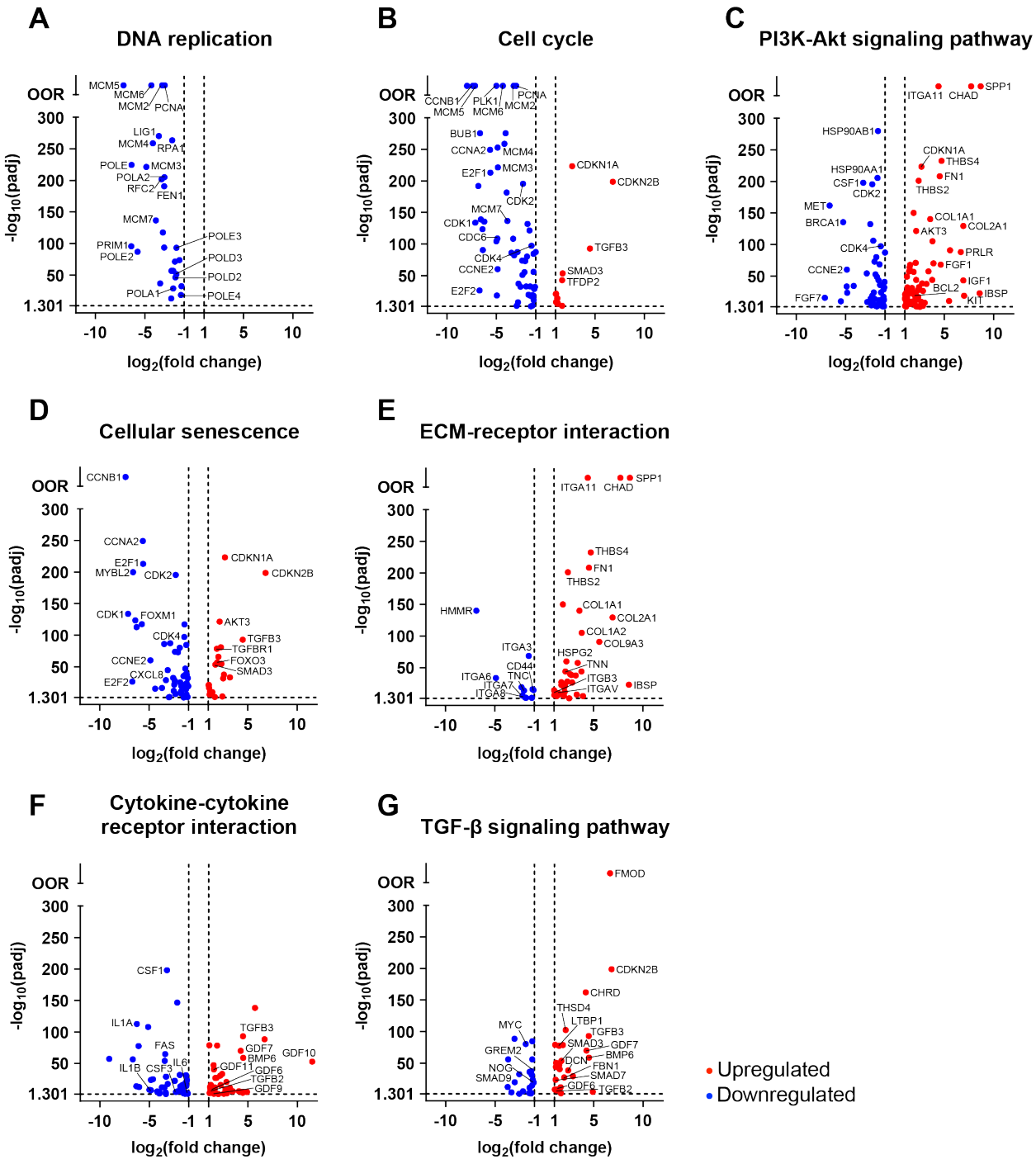


**Figure 5. TGF-β1 vs. FBS: Proliferation related genes are significantly downregulated, and genes involved in cell-ECM interactions and cytokine signaling are upregulated in myofibroblasts compared to fibroblasts.** (A-G) Volcano plots represent individual genes significantly up- or downregulated within selected KEGG pathways from the comparison of myofibroblasts to fibroblasts. Genes with padj ≤ 0.05 (horizontal dashed line) and | log2(fold change) | ≥ 1 (vertical dashed lines) were considered significant. Red dots indicate genes that were upregulated in myofibroblasts

927 while blue dots indicate downregulated genes. Genes generally associated with either
928 TGF-β1 or FBS induced phenotypes and several other significant genes with high padj
929 values or fold changes have been labeled.

930

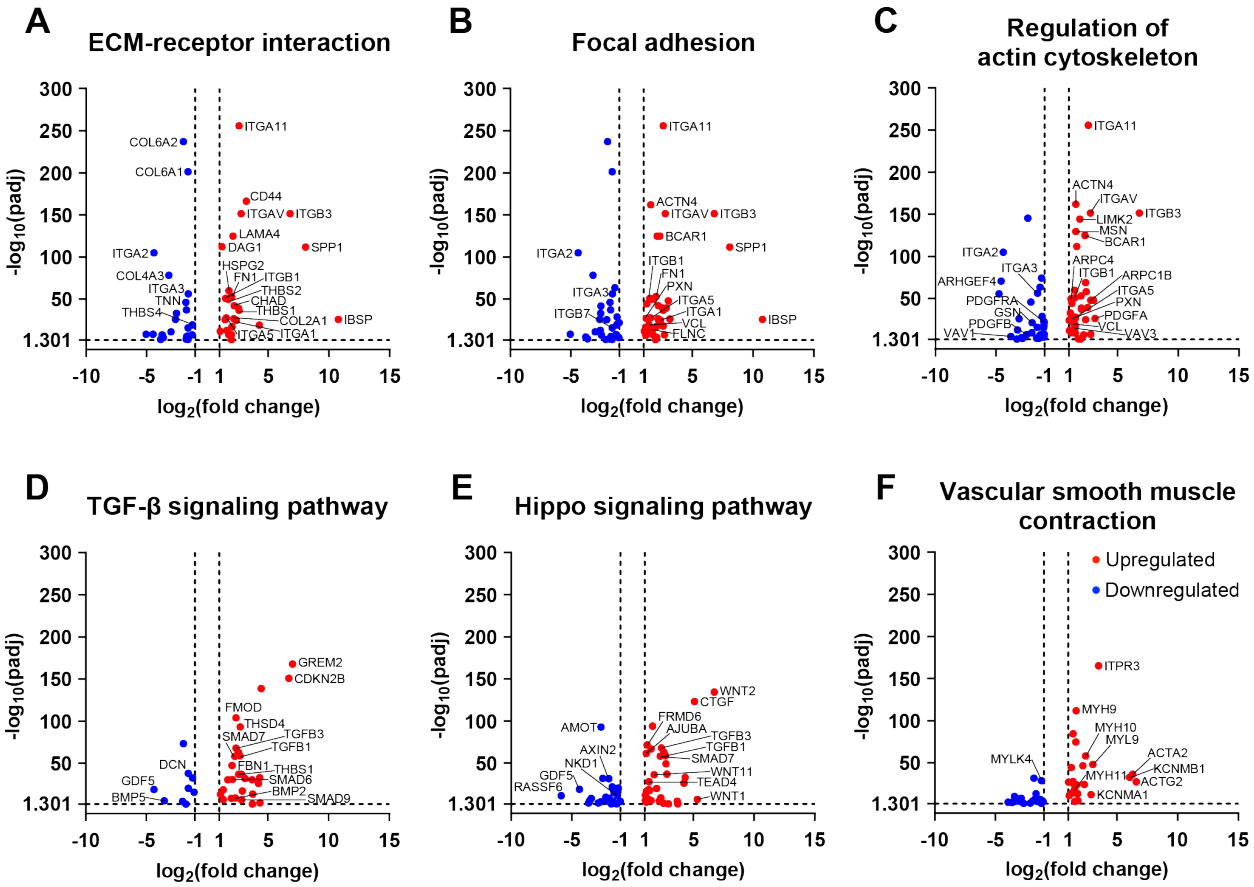


**Figure 6. TGF-β1 vs. SF: Genes in KEGG pathways related to cell-ECM interactions and mechanotransduction are differentially expressed in myofibroblasts compared to keratocytes.** (A-F) Volcano plots represent individual genes significantly up- or downregulated within selected KEGG pathways from the comparison of myofibroblasts to keratocytes. Genes with padj ≤ 0.05 (horizontal dashed line) and | log2(fold change) | ≥ 1 (vertical dashed lines) were considered significant. Red dots indicate genes that were upregulated in myofibroblasts while blue dots indicate downregulated genes. Genes generally associated with TGF-β1 induced myofibroblast phenotypes and several other significant genes with a high padj values or fold changes have been labeled.

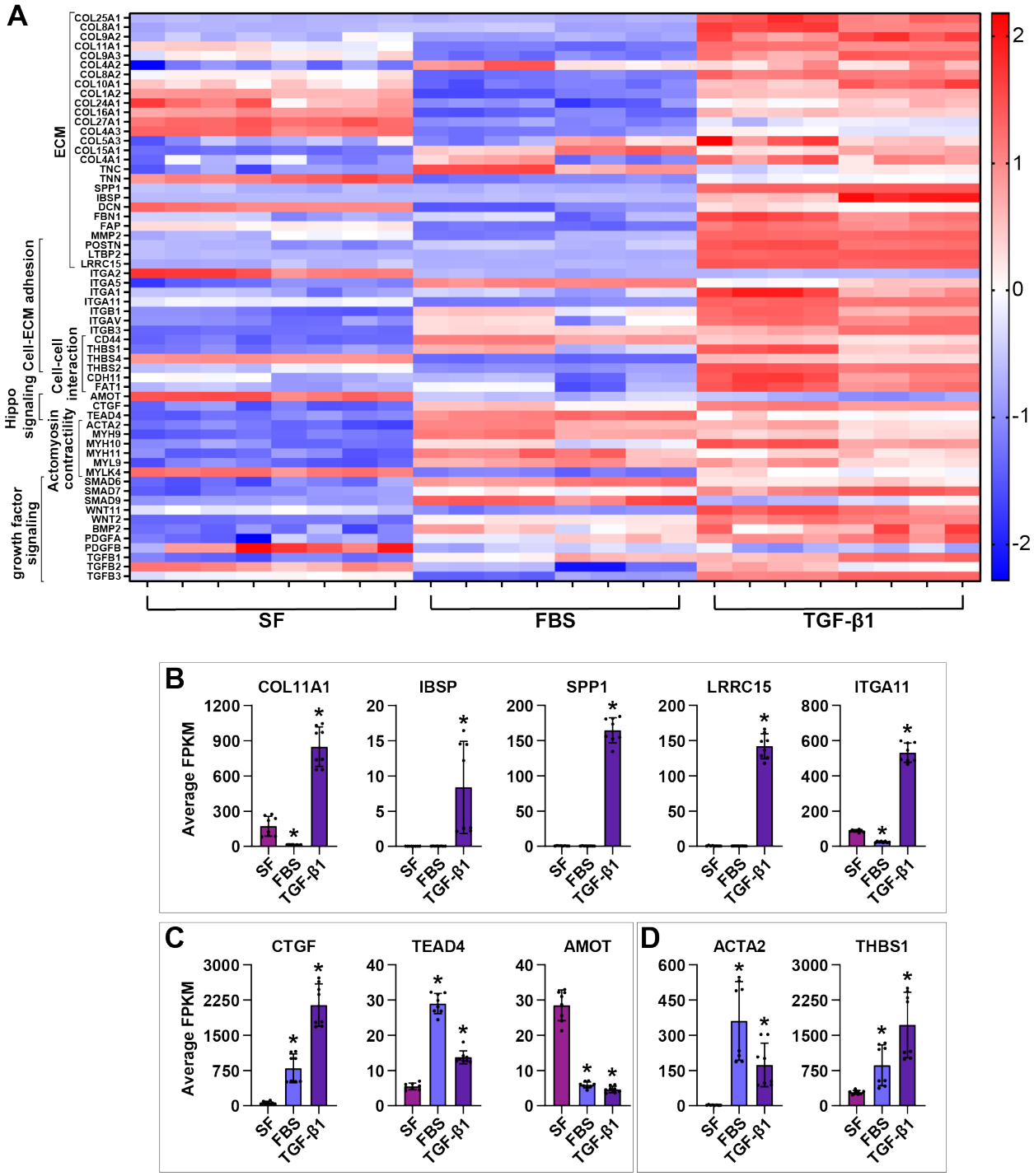


**Figure 7. Myofibroblast differentiation is associated with specific ECM and Hippo signaling related genes.** (A) Heatmap of normalized, log2-transformed FPKM values (log2(FPKM+1)) for several genes associated with ECM, cell-cell interactions, Hippo signaling, actomyosin contractility, and growth factor signaling that were differentially expressed in myofibroblasts compared to either keratocytes or fibroblasts. Red color indicates genes with high relative expression levels and blue color indicates genes with

949 lower expression levels. Selected genes associated with (B) ECM, (C) Hippo signaling,
950 and (D) myofibroblast differentiation have been highlighted in the bar plots. The average
951 FPKM values have been indicated for comparison among the three culture conditions.
952 Asterisks indicate if expression levels in either FBS or TGF-β1 conditions were found to
953 be significantly different with respect to SF based on the differential expression analysis
954 (padj ≤ 0.05 and | log2(fold change) | ≥ 1).

955

956 **Supplemental figures**

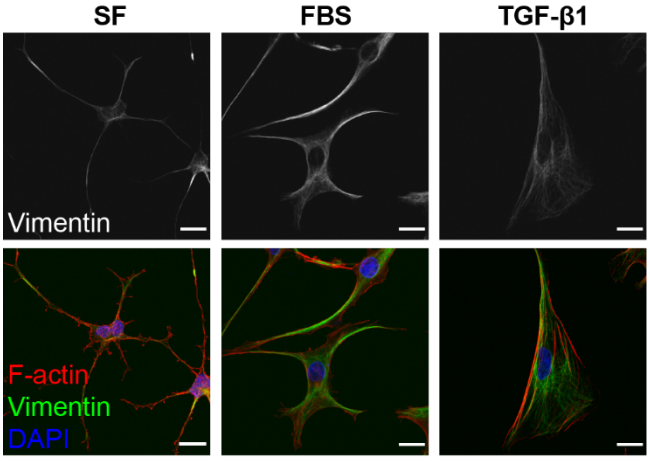


957

958 **Figure S1.** Confocal images of vimentin immunofluorescence and vimentin overlaid with
959 F-actin and DAPI for corneal keratocytes in SF conditions, or in the presence of FBS or
960 TGF-β1. Scale bar = 20 $\mu$m.

961

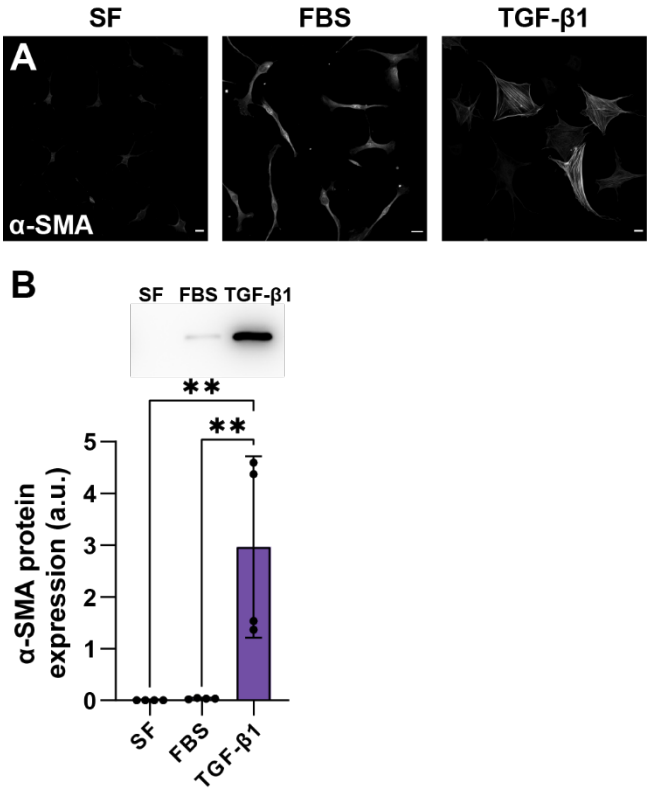


**Figure S2.** (A) Confocal images of alpha-smooth muscle actin (α-SMA) immunofluorescence for corneal keratocytes in SF, FBS, or TGF-β1 conditions. Scale bar = 20 $\mu$m. (B) Representative western blot and quantification of α-SMA expression across culture conditions. Quantification of target protein expression was normalized to total protein and reported in arbitrary units (a.u.). Error bars represent mean ± s.d. for 4 experimental replicates. A one-way ANOVA with a Tukey post-hoc test was used to compare group means (**, $p < 0.01$).

| | TGF-β1 vs. SF | FBS vs. SF |
|---|---|---|
| **GENES** | **padj** | **padj** |
| COL11A1 | 6.00E-17 | 5.22E-48 |
| IBSP | 9.64E-27 | ns |
| SPP1 | 1.48E-112 | ns |
| LRRC15 | 2.97E-78 | ns |
| ITGA11 | 2.34E-256 | 1.11E-72 |
| CTGF | 9.51E-124 | 3.41E-42 |
| TEAD4 | 1.73E-28 | 3.85E-110 |
| AMOT | 1.45E-93 | 3.34E-79 |
| ACTA2 | 5.52E-37 | 8.79E-53 |
| THBS1 | 1.66E-37 | 6.93E-10 |

970 **Table S1.** Significance values of genes differentially expressed in the presence of FBS
971 or TGF-β1 compared to SF, represented as padj values. List of genes included are those
972 represented as bar plots in Fig. 7B-D.

973